9 Interlayer Exchange Interactions in Magnetic Multilayers

P. Bruno

in "Magnetism: Molecules to Materials III Nanosized Magnetic Materials" edited by Joel S. Miller and Marc Drillon (WILEY-VCH, Weinheim, 2002)

9.1 Introduction

Magnetic multilayers typically consist of alternate stacks of ferromagnetic and non-ferromagnetic spacer layers. The typical thickness of an individual layer ranges between a few atomic layers (AL) to a few tens of AL. The magnetic layers usually consist of elemental metallic ferromagnets (Fe, Co, Ni) or alloys thereof (e. g. permalloy). The spacer layers can consist of any transition or noble metal; they are either paramagnetic (Cu, Ag, Au, Ru, Pd, V, etc.) or antiferromagnetic (Cr, Mn).

Because of the spacer layers, the magnetic layers are, to first approximation, magnetically decoupled from each other, i. e. their basic magnetic properties such as magnetization, Curie temperature, magnetocrystalline anisotropy, magneto-optical response, etc., are essentially those of an individual layer. This approximation, however, is not sufficient for accurate descrition of the magnetism of multilayers, and one must consider the magnetic interactions which couple successive magnetic layers through spacer layers.

The various interactions giving rise to an interlayer magnetic interaction are: (i) the dipolar interaction and (ii) the indirect exchange interaction of the Ruderman–Kittel–Kasuya–Yosida (RKKY) type.

For a homogeneously magnetized layer consisting of a continuous medium, there is no dipolar stray field, so that dipolar interlayer coupling can arise only as a result of departures from this idealized situation. This is the case when one considers the real crystalline structure of the layer. It is, however, easy to show that the dipolar stray field decays exponentially as a function of the distance from the magnetic layer, with a decay length of the order of the lattice parameter, so that this effect is completely negligible compared with the interaction as a result of exchange, to be discussed below. Significant dipolar interlayer interactions can, nevertheless, arise from correlated roughness imperfections of the layers ("orange peel" effect) as first pointed out by Néel [1]. This effect, however, becomes negligible for the high quality multilayers that can be fabricated nowadays. Finally, dipolar interactions are important when the magnetic layers are not saturated and split into magnetic domains; this interaction leads in particular to a correlation between the magnetic domains of the successive magnetic layers. This phenomenon is, therefore, extrinsinc and we shall disregard it below by restricting ourselves to homogeneously magnetized layers.

The indirect exchange interaction has a completely different physical origin. It is mediated by conduction electrons which are scattered successively by the mag-

netic layers. Historically, this type of interaction was first proposed by Ruderman and Kittel to describe the indirect interactions between nuclear spins in a metal [2], and then extended to electronic magnetic moments by Kasuya [3] and Yosida [4]. This interaction has received a much attention, in particular in the context of dilute magnetic alloys. Neither theoretical predictions, nor the experiment results, were, however, sufficiently precise to enable fully understanding of this mechanism and quantitative testing of the theoretical predictions. Indirect exchange interactions have received intensly renewed attention since 1990 in the context of magnetic multilayers – indeed, in contrast with the situation of a dilute alloy, in which the distance between magnetic impurities is randomly distributed, multilayers enable controlled variation of the distance between successive magnetic layers and their crystallographic orientation; this enables a very detailled study of indirect exchange interactions.

In this chapter we present an overview of the state-of-the-art of our understanding of interlayer coupling as a result of indirect exchange interactions in transition metal multilayers. In Section 2 we give a short overview of the experimental observations. This is followed by an overview of the theoretical approaches that have been used to describe the interlayer exchange coupling (Section 3). Theoretical description based upon the idea of spin-dependent quantum confinement is presented in Section 4. The behavior obtained in the limit of large spacer thickness is discussed in Section 5, and the dependence of interlayer exchange coupling on magnetic layer thickness and on overlayer thickness are treated in Sections 6 and 7, respectively. The amplitude and phase of interlayer coupling oscillations are discussed in Section 8.

9.2 Survey of Experimental Observations

Interlayer magnetic interactions were first reported in rare-earth superlattices [5, 6]. Rare-earth multilayers will not, however, be considered here, and the reader is refered to recent review papers on this subject [7, 8].

For transition metals systems, antiferromagnetic interlayer exchange coupling in Fe/Cr/Fe layers was first reported by Grünberg et al. [9]. They observed an antiferromagnetic interlayer interaction, decaying regularly with increasing Cr spacer thickness. Phenomenologically, the interlayer interaction energy per unit area can be expressed as

$$E(\theta) = J \cos\theta, \tag{1}$$

where θ is the angle between the magnetizations of the two magnetic layers, and J is called the interlayer coupling coupling constant. With the sign convention adopted here, a positive (negative) value of J relates to an antiferromagnetic (ferromagnetic) type of coupling. One should pay attention to the fact that other conventions for the sign and normalization of the coupling constant are frequently found in the literature.

In practice, an antiferromagnetic interlayer interaction is easily revealed and measured by performing a magnetization measurement (or measurement of any property proportional to the magnetization, for example magneto-optical Kerr or Faraday effect) as a function of an applied magnetic field. In zero field, because of the antiferromagnetic interaction, the magnetization of successive magnetic layers is antiparallel to each other, resulting in zero remanent magnetization (if the magnetic moments of the layers are equivalent). When an external field is applied the Zeeman energy tends to align the magnetization of both layers in the field direction, so that the magnetization progressively increases until a saturation field is reached; the value of the latter gives a quantitative measure of the antiferromagnetic interaction strength. One should be aware, however, that it is not always easy to distinguish this behavior from the effect of magnetocrystalline anisotropy, or magnetic domains. Hence, for a convincing measurement it is necessary to perform a quantitative micromagnetic analysis of the influence of the latter effects [10, 11].

A ferromagnetic interaction is much more difficult to detect and measure quantitatively, because the application of an external magnetic field has no direct action on the mutual orientation of the magnetizations of the successive magnetic layers and thus cannot probe their mutual interaction. It is, nevertheless, possible to measure ferromagnetic interlayer interactions by means of magnetometry by using specially devised structures. This can be achieved by pinning the magnetization of one magnetic layer, leaving the other one free to align itself along an external magnetic field. The pinning of the magnetization of a ferromagnetic layer can be achieved by coupling it to an antiferromagnetic layer [12], or by coupling it to another ferromagnetic layer via a strong antiferromagnetic coupling [13], or by using a magnetic layer with a strong magnetic anisotropy and coercivity [14].

The discovery, by Parkin et al. [15], of spectacular oscillatory variation of the interlayer coupling depending on spacer layer thickness in Fe/Cr and Co/Ru multilayers has stimulated intense research activity in this field. Systematic studies by Parkin revealed, furthermore, that the oscillatory behavior is observed for spacer layers consisting of almost any transition or noble metal and is therefore essentially a universal feature of this phenomenon [16].

The generic behavior of oscillatory interlayer exchange coupling is an interaction which oscillates periodically in sign and magnitude, with an amplitude which decays as $1/D^2$, where D is the spacer thickness. The oscillation periods depend on the nature and crystalline orientation of the spacer metal, but not on the nature or thickness of the magnetic layers. Typical values of oscillation periods are between 2 and 10 AL. The strength of the interaction, on the other hand, depends both on the characteristics of the spacer and of the magnetic layers.

To enable very precise investigation of the dependence on thickness of the interlayer coupling and to avoid problems resulting from unsufficient reproducibility in sample growth conditions and layer thicknesse, Fuss et al. [17] introduced a new technique, which consists in using samples in which the spacer is prepared as a wedge of continuously varying (average) thickness, obtained by moving a shutter close to the sample during deposition. By using Kerr effect, magnetometry can be performed locally by scanning a focused laser on the sample. This ingenious method turned out

to be essential for successfully revealing full richness of thickness variation of the interlayer exchange coupling.

In particular, in confirmation of theoretical predictions (see below) it has been found experimentally that multiperiodic oscillatory coupling exists in Fe/Au(001)/Fe [17–19], Co/Cu(001)/Co [20–22], and Fe/Ag(001)/Fe [23] multilayers.

The dependence on spacer thickness of the coupling constant J can therefore generally be expressed as:

$$J = \sum_{\alpha} \frac{A_\alpha}{D^2} \sin(q_\alpha D + \phi_\alpha) \tag{2}$$

where the index α labels the various oscillatory components. The strength of interlayer exchange coupling, as expressed by A_α (which the dimension of an energy), is typically of the order of 1 to 10 meV, which (for a spacer thickness of 1 nm) corresponds to a value of the order of 0.1 to 1 mJ m^{-2} for the coupling constant J.

Although the greatest dependence on thickness is the dependence on spacer layer thickness, (weak) oscillatory dependence on magnetic layer thickness has been observed for the Co/Cu(001)/Co system by Bloemen et al. [24] and for the Fe/Cu(001)/Co system by Back et al. [25], and dependende on the thickness of a non-magnetic coverage layer has been observed for the Co/Cu(001)/Co system by de Vries et al. [26], for the Fe/Au(001)/Fe system by Okuno and Inomata [27], and for the Co/Au(111)/Co system by Bounouh et al. [28], in accordance with theoretical predictions (see below for a detailed discussion).

Although the most frequent behavior for the interlayer exchange coupling is of the form given by Eq. (1), Rührig et al. [29] have observed in the Fe/Cr(001)/Fe system a special kind of coupling in which the magnetization of successive magnetic layers tends to be perpendicular to each other, rather than either parallel or antiparallel, as follows from Eq. (1). This behavior can be understood if one assumes that the coupling is of the form

$$E(\theta) = J_1 \cos\theta + J_2 \cos^2\theta \tag{3}$$

In combination with the effect of cubic magnetocrystalline anisotropy, the above coupling can, indeed, lead to a 90 degree configuration for suitable values of the coupling constants J_1 and J_2. This effect has been observed in other systems also. This additional coupling contribution is often dubbed "biquadratic" coupling. Although such coupling can, in principle, arise from intrinsic mechanism, this effect is usually too small to explain the experimental observations, and it is believed that other (extrinsic) mechanisms related to structural defects are responsible. This effect will not be considered further in this paper; the interested reader can find up-to-date discussions on this topic in recent review papers [30, 31].

Note that interlayer exchange coupling has been observed not only for metallic spacer layers, but also for semiconducting spacer layers [32–35]. This effect is, however, believed to have a mechanism different from that operating for metallic spacer layers, and will not be discussed further here.

9.3 Survey of Theoretical Approaches

9.3.1 RKKY Theory

The striking similarity between the oscillatory behavior observed experimentally and that obtained from the RKKY interaction between magnetic impurities suggests, of course, that the two phenomena have a common mechanism. This prompted researchers to attempt to describe interlayer exchange coupling by adapting the RKKY theory [36–40].

This approach rapidly achieved significant success. In particular, Yafet [36] first explained the oscillatory behavior and the $1/D^2$ decay law (compared with a $1/D^3$ decay obtained for the RKKY interaction between impurities). Extending the theory to take proper account of the real electronic structure of the spacer material (as opposed to the free electron approximation used so far), Bruno and Chappert [38, 39] derived the selection rule giving the oscillation period(s) of the oscillatory coupling in terms of the (bulk) Fermi surface of the spacer. By applying this selection rule, they calculated the oscillation periods for noble metal spacers; their results (including the prediction of multiperiodic oscillations) were soon confirmed quantitatively by experiment (see discussion below), giving strong support to the RKKY theory. Because of the approximations used, however, the RKKY theory did not enable quantitative description the amplitude and phase of the oscillatory coupling.

9.3.2 Quantum Well Model

Independently, an (apparently) different mechanism was soon proposed by Edwards et al. [41] and by other authors [42–45]. In this approach the coupling is ascribed to the change of density of states resulting from the spin-dependent confinement of the electrons (or holes) in the quantum well provided by the spacer layer. Remarkably, this approach yielded exactly the same oscillatory behavior and decay as the RKKY interaction. On the other hand, the description of the amplitude and phase was more satisfactory, although early attempts to calculate these were based on assumptions that were too crude (free electron model, single tight-binding model) to yield realistic quantitative results. More realistic calculations have subsequently been performed on the basis of the quantum-well model [46–48].

9.3.3 *sd*-Mixing Model

Yet another approach was based upon the *sd*-mixing model [49–51], proposed earlier by Anderson [52] and Caroli [53] to described the interaction between magnetic impurities in metals. This approach yielded the same result as the RKKY theory for the oscillation periods and decay law of the coupling. Description of the amplitude and phase of the coupling was more physical than that provided by the RKKY theory. Bruno [51], in particular, showed that the amplitude and phase in terms of a (suitably

adapted) Friedel sum rule [54] for the magnetization and charge of an the magnetic "impurities."

9.3.4 Unified Picture in Terms of Quantum Interferences

The coexistence of a variety of apparently different mechanisms predicting essentially similar behavior for the coupling led to a somewhat puzzling and controversial situation regarding the true nature of the mechanism of interlayer exchange coupling. This puzzle was solved when Bruno [55, 56] and subsequently Stiles [57] showed that the different approaches indeed corresponded to different approximations of a same mechanism. They reformulated it in a physically appealing picture in which the amplitude and phase of the oscillatory coupling are expressed in terms of the amplitude and phase of reflection coefficients for the electrons at the interfaces between the spacer and the magnetic layers.

This approach has been used by several authors to perform quantitative calculations for realistic systems [58–60].

Furthermore, thanks to its physical transparency, this approach has enabled qualitative prediction of new behavior, for example oscillations depending on magnetic layer thickness [61] and on overlayer thickness [62].

9.3.5 First-principles Calculations

Finally, numerous authors have performed first-principles calculations of interlayer exchange coupling for realistic systems [63–72]. Besides modeling the approaches mentioned above, first-principles calculation plays a very important rôle in elucidating the mechanism of interlayer exchange coupling: on one hand, it provides a test of the qualitative predictions of the simplified models, while on the other hand it yields quantitative predictions for realistic systems than can be compared critically with experimental observations. The most widely investigated system is the Co/Cu/Co(001) system, which has served as a benchmark for the theory of interlayer exchange coupling. While early attemps yielded doubtful results, essentially because of the great difficulty of such numerical calculation, the most recent results have given results than can be considered satisfactory in many respects (see discussion below).

9.4 Quantum Confinement Theory of Interlayer Exchange Coupling

The purpose of this section is to present as simply as possible the mechanism of interlayer exchange coupling in terms of quantum interferences as a result of electron confinement in the spacer layer. The emphasis here will be on physical concepts rather than on mathematical rigor. This discussion is based on that given in Ref. [74].

9.4.1 Elementary Discussion of Quantum Confinement

For the sake of clarity, we shall first consider an extremely simplified model, namely the one-dimensional quantum well, which nevertheless contains the essential physics involved in the problem. We shall then progressively refine the model to make it more realistic.

The model consists in a one-dimensional quantum well representing the spacer layer (of potential $V = 0$ and width D), sandwiched between two "barriers" A and B of respective widths L_A and L_B, and respective potentials V_A and V_B. Note that we use the term "barrier" in a general sense, i. e., V_A and V_B are not necessarily positive. The barrier widths, L_A and L_B, can, furthermore, be finite or infinite, without any restriction.

9.4.1.1 Change of the Density of States as a Result of Quantum Interferences

Let us consider an electron of wavevector k^+ (with $k^+ > 0$) propagating towards the right in the spacer layer; as this electrons arrives at barrier B, it is partially reflected to the left, with a (complex) amplitude $r_B \equiv |r_B|e^{i\phi_B}$. The reflected wave of wavevector k^- is in turn reflected from barrier A with an amplitude $r_A \equiv |r_A|e^{i\phi_A}$, an so on. (For the one-dimensional model, of course, $k^- = -k^+$; this property will, however, generally not be true for three-dimensional systems to be studied below.) The module $|r_{A(B)}|$ of the reflection coefficient expresses the magnitude of the reflected wave, whereas the argument $\phi_{A(B)}$ represents the phase shift resulting from the reflection (note that the latter is not absolutely determined and depends on the choice of the coordinate origin).

The interferences between the waves as a result of the multiple reflections on the barriers induce a modification of the density of states in the spacer layer, for the electronic state under consideration. The phase shift resulting from a complete round trip in the spacer is

$$\Delta\phi = qD + \phi_A + \phi_B \tag{4}$$

with

$$q \equiv k^+ - k^- \tag{5}$$

If the interferences are constructive, i. e., if:

$$\Delta\phi = 2n\pi \tag{6}$$

where n is an integer, one has an increase in the density of states; conversely, if the interferences are destructive, i. e., if

$$\Delta\phi = (2n + 1)\pi \tag{7}$$

one has a reduction in the density of states. Thus, to a first approximation, we expect the modification of the density of states in the spacer, $\Delta n(\varepsilon)$, to vary with D in the manner:

$$\Delta n(\varepsilon) \approx \cos\left(qD + \phi_A + \phi_B\right). \tag{8}$$

We expect, furthermore, that this effect will proportional to the amplitude of the reflections at barriers A and B, i. e., to $|r_A r_B|$; finally, $\Delta n(\varepsilon)$ must be proportional to the width, D, of the spacer and to the density of states per unit energy and unit width:

$$\frac{2}{\pi}\frac{\mathrm{d}q}{\mathrm{d}\varepsilon} \tag{9}$$

which includes a factor of 2 for spin degeneracy. We can also include the effect of higher-order interferences, because of n round trips in the spacer; the phase shift $\Delta\phi$ is then multiplied by n and $|r_A r_B|$ is replaced by $|r_A r_B|^n$. Gathering all the terms, we obtain:

$$\begin{aligned}
\Delta n(\varepsilon) &\approx \frac{2D}{\pi}\frac{\mathrm{d}q}{\mathrm{d}\varepsilon}\sum_{n=1}^{\infty}|r_A r_B|^n \cos n\left(qD + \phi_A + \phi_B\right) \\
&= \frac{2}{\pi}\,\mathrm{Im}\left(\mathrm{i}D\frac{\mathrm{d}q}{\mathrm{d}\varepsilon}\sum_{n=1}^{\infty}(r_A r_B)^n\,\mathrm{e}^{niqD}\right) \\
&= \frac{2}{\pi}\,\mathrm{Im}\left(\mathrm{i}\frac{\mathrm{d}q}{\mathrm{d}\varepsilon}\frac{r_A r_B\,\mathrm{e}^{iqD}}{1 - r_A r_B\,\mathrm{e}^{iqD}}\right)
\end{aligned} \tag{10}$$

As will appear clearly below, it is more convenient to consider the integrated density of states:

$$N(\varepsilon) \equiv \int_{-\infty}^{\varepsilon} n(\varepsilon')\,\mathrm{d}\varepsilon'. \tag{11}$$

The modification $\Delta N(\varepsilon)$ of the integrated density of states because of electron confinement is:

$$\begin{aligned}
\Delta N(\varepsilon) &= \frac{2}{\pi}\,\mathrm{Im}\sum_{n=1}^{\infty}\frac{(r_A r_B)^n}{n}\,\mathrm{e}^{niqD} \\
&= -\frac{2}{\pi}\,\mathrm{Im}\,\ln\left(1 - r_A r_B\,\mathrm{e}^{iqD}\right)
\end{aligned} \tag{12}$$

A simple graphical interpretation of the above expression can be obtained by noting that $\mathrm{Im}\,\ln(z) = \mathrm{Arg}\,(z)$, for z complex; thus, $\Delta N(\varepsilon)$ is given by the argument, in the complex plane, of a point located at an angle $\Delta\phi = qD + \phi_A + \phi_B$ on a circle of radius $|r_A r_B|$ centred in Fig. 1. This graphical construction is shown in Fig. 1.

The variation of $\Delta N(\varepsilon)$ as a function of D is shown in Fig. 2, for different values of the confinement strength $|r_A r_B|$. For weak confinement (a), $\Delta N(\varepsilon)$ varies with D in sinusoidal manner. As one the confinement strength is increased (b), the oscillations are distorded, because of higher-order interferences. Finally, for full confinement (c), $\Delta N(\varepsilon)$ contains jumps that correspond to the appearance of bound states. We note, however, that the period, Λ, of the oscillations of $\Delta N(\varepsilon)$ does not depend on the confinement strength, but only on the wavevector $q \equiv k^+ - k^-$, i. e. $\Lambda = 2\pi/q$.

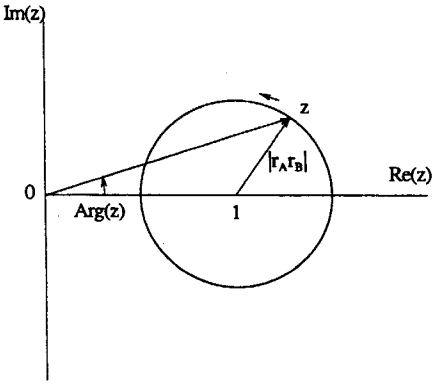

Fig. 1. Graphical interpretation of Eq. (12).

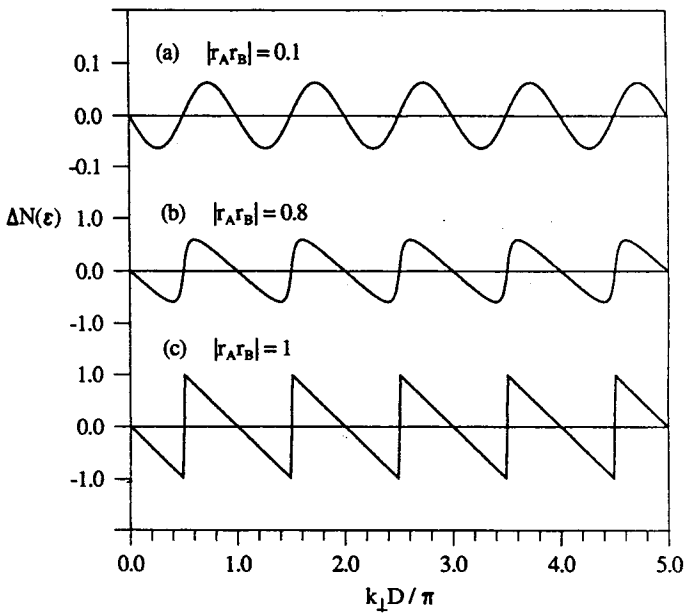

Fig. 2. Variation of $\Delta N(\varepsilon)$ as a function of D, for different values of the confinement strength: (a) $|r_A r_B| = 0.1$, (b) $|r_A r_B| = 0.8$, (c) $|r_A r_B| = 1$ (full confinement). Note the different scales along the ordinate axis.

So far, we have implicitely restricted ourselves to positive energy states. Negative energy states (i. e., of imaginary wavevector) are forbidden in the absence of barriers A and B, because their amplitude diverges either on the right or on the left, so that they cannot be normalized. This matter of fact is no longer-true in the presence of the barriers if V_A (or V_B, or both V_A and V_B) is negative – the negative energy states, i. e. varying exponentially in the spacer, can be connected to allowed states of A or B. To treat these states consistently we simply have to extend the concept of reflection

coefficient to states of an imaginary wavevector, which is straightforward. One can check that, with this generalization, Eq. (12) acounts properly for the contribution of the evanescent states. Physically, this can be interpretated as coupling of A and B by a tunnel effect [73, 74].

9.4.1.2 Energy Associated with the Quantum Interferences in the Spacer

Let us now study the modification of the energy of the system which results from the quantum interferences. To conserve the total number of electrons it is convenient to work within the grand-canonical ensemble, and to consider the thermodynamic grand-potential, which is given by:

$$\begin{aligned}\Phi &\equiv -k_B T \int_{-\infty}^{+\infty} \ln\left[1+\exp\left(\frac{\varepsilon_F-\varepsilon}{k_B T}\right)\right] n(\varepsilon)\,\mathrm{d}\varepsilon \\ &= -\int_{-\infty}^{+\infty} N(\varepsilon)\, f(\varepsilon)\,\mathrm{d}\varepsilon. \end{aligned} \tag{13}$$

At $T = 0$, this reduces to:

$$\begin{aligned}\Phi &\equiv \int_{-\infty}^{\varepsilon_F} (\varepsilon-\varepsilon_F)\, n(\varepsilon)\,\mathrm{d}\varepsilon \\ &= -\int_{-\infty}^{\varepsilon_F} N(\varepsilon)\,\mathrm{d}\varepsilon \end{aligned} \tag{14}$$

The energy ΔE associated with the interferences is the contribution to Φ corresponding to $\Delta N(\varepsilon)$:

$$\Delta E = \frac{2}{\pi}\,\mathrm{Im}\int_{-\infty}^{+\infty} \ln\left(1 - r_A r_B\, \mathrm{e}^{\mathrm{i}qD}\right)\,\mathrm{d}\varepsilon. \tag{15}$$

9.4.1.3 Three-dimensional Layered System

Generalization of the above discussion to the more realistic case of a three-dimensional layered system is immediate. Because the system is invariant by translation parallel to the plane, the in-plane wavevector $\mathbf{k}_\parallel$ is a good quantum number. Thus, for a given $\mathbf{k}_\parallel$, one has an effective one-dimensional problem analogous to that discussed above. The resulting effect of quantum intereferences is obtained by summing on $\mathbf{k}_\parallel$ over the two-dimensional Brillouin zone. The modification of the integrated density of states per unit area is:

$$\Delta N(\varepsilon) = -\frac{1}{2\pi^3}\,\mathrm{Im}\int \mathrm{d}^2\mathbf{k}_\parallel \ln\left(1 - r_A r_B\, \mathrm{e}^{\mathrm{i}q_\perp D}\right) \tag{16}$$

and the interference energy per unit area is:

$$\Delta E = \frac{1}{2\pi^3}\,\mathrm{Im}\int \mathrm{d}^2\mathbf{k}_\parallel \int_{-\infty}^{+\infty} f(\varepsilon) \ln\left(1 - r_A r_B\, \mathrm{e}^{\mathrm{i}q_\perp D}\right)\,\mathrm{d}\varepsilon \tag{17}$$

9.4.1.4 Quantum Size Effect in an Overlayer

A thin overlayer deposited on a substrate is a system of considerable interest. One of the barriers (say, A) is the vacuum, and barrier B is the substrate itself. The potential of the vacuum barrier is $V_{vac} = \varepsilon_F + W$, where W is the the work function; thus it is perfectly reflecting for occupied states, i. e. $|r_{vac}| = 1$. The reflection on the substrate (or coefficent r_{sub}) can, on the other hand, be total or partial, depending on the band matching for the state under consideration.

The spectral density of the occupied states in the overlayer can be investigated experimentally by photoemission spectroscopy; in addition, by using inverse photoemission one can study the unoccupied states. If, furthermore, these techniques are used in the "angle-resolved" mode, they give information about the spectral density *locally in the* $\mathbf{k}_\parallel$ *plane.*

For an overlayer of given thickness, the photoemission spectra (either direct or inverse) contain maxima and minima corresponding, respectively, to the energies for which the interferences are constructive and destructive. When the confinement is total, narrow peaks can be observed; these correspond to the quantized confined states in the overlayer, as was pointed out by Loly and Pendry [75].

Quantum size effects arising because of electron confinement in the photoemission spectra of overlayers have been observed in a variety of non-magnetic systems [76–84]. The systems Au(111)/Ag/vacuum and Cu(111)/Ag/vacuum, in particular, are excellent examples of this phenomenon [81, 83].

9.4.1.5 Paramagnetic Overlayer on a ferromagnetic Substrate – Spin-polarized Quantum Size Effect

So far our discussion has been concerned with non-magnetic systems exclusively. Qualitatively new behavior can be expected when some of the layers are ferromagnetic. An example of particular interest is that of a paramagnetic overlayer on a ferromagnetic substrate.

In the interior of the overlayer the potential is independent of the spin; the propagation of electrons is, therefore, described by a wavevector $k_\perp$, which is spin-independent. The reflection coefficient on the vacuum barrier, r_{vac}, is also spin-independent. The ferromagnetic substrate, however, constitutes a spin-dependent potential barrier; thus the substrate reflection coefficients for electrons with a spin parallel to the majority and minority spin directions of the substrate are, respectively, $r_{sub}^{\uparrow}$ and $r_{sub}^{\downarrow}$. It is convenient to define the spin average:

$$\bar{r}_{sub} \equiv \frac{r_{sub}^{\uparrow} + r_{sub}^{\downarrow}}{2} \tag{18}$$

and the spin asymmetry:

$$\Delta r_{sub} \equiv \frac{r_{sub}^{\uparrow} - r_{sub}^{\downarrow}}{2}. \tag{19}$$

In this case the electron confinement in the overlayer gives rise to a spin-dependent modulation of the spectral density as the overlayer thickness is changed; the period of the modulation is the same for both spins, whereas the amplitude and phase are expected to be spin-dependent.

The quantum size effects in paramagnetic overlayers on a ferromagnetic substrate have been investigated by several groups [85–98]. The systems studied most are Cu overlayers on a Co(001) substrate and Ag overlayers on a Fe(001) substrate. Ortega and Himpsel [86, 87] observed a quantum size effect in the normal-emission photoelectron spectra of a copper overlayer on a fcc cobalt (001) substrate. They observed peaks arising as a result of quantum size effects, and an oscillation of the photoemission intensity in both, the photoemission and in the inverse photoemission spectra. These quantum size effects manifest themselves also in the form of oscillatory behavior in the photoemission intensity at the Fermi level; because the observed oscillation period (5.9 atomic layers) is close to the long period of interlayer exchange coupling oscillations in Co/Cu(001)/Co, it was suggested that the two phenomena should be related to each other: Ortega and Himpsel also claimed that the observed oscillations in photoemission are spin-dependent and mostly arise from minority electrons. This conjecture has been confirmed directly, by Garrison et al. [89] and by Carbone et al. [90], independently, by means of spin-polarized photoemission. They found that both the intensity and the spin-polarization have oscillatory behavior with the same period (5–6 atomic layers) but opposite phases; this indicates that the quantum-size effect does indeed take place predominantly in the minority-spin band, as proposed by Ortega and Himpsel [86, 87]. Kläsges et al. [96] and Kawakami et al. [98] have recently observed spin-polarized quantum-size effects in a copper overlayer on cobalt (001) for a non-zero, in-plane wavevector corresponding to the short period oscillation of interlayer exchange coupling in Co/Cu(001)/Co; they observed short-period oscillations of the photoemission intensity, in good agrement with the short-period oscillations of interlayer coupling. This observation provides a further confirmation of the relationship between quantum-size effects in photoemission and oscillation of interlayer exchange coupling.

Photoemission studies of quantum size effects have also been performed on other types of system, e. g. a ferromagnetic overlayer on a non-magnetic substrate, or systems comprising more layers [99–103].

Photoemission spectroscopy undoubtedly constitutes a method of choice for investigating quantum-size effects in metallic overlayers; this is because its unique features enable selectivity in energy, in-plane wavevector, and spin.

Besides photemission, spin-polarized quantum-size effects in paramagnetic overlayers on a ferromagnetic substrate also cause oscillatory behavior (which depends on overlayer thickness) of spin-polarized secondary electron emission [104, 105], linear [106–111], and non-linear [112, 113] magneto-optical Kerr effect, and magnetic anisotropy [114, 115]. These effects usually, however, involve a summation over all electronic states, and so quantitative analysis of these quantum-size effects may be fairly complicated.

9.4.2 Interlayer Exchange Coupling Because of Quantum Interferences

Let us now consider a paramagnetic layer sandwiched between two ferromagnetic barriers A and B. The reflection coefficients on both sides of the paramagnetic spacer layer are now spin dependent. A priori the angle, θ, between the magnetizations of the two ferromagnetic barriers can take any value; for the sake of simplicity, however, we shall restrict ourselves here to the ferromagnetic (F) (i.e. $\theta = 0$) and the antiferromagnetic (AF) (i. e. $\theta = \pi$) configurations.

For the ferromagnetic configuration, the energy change per unit area because of quantum interference is easily obtained from Eq. (17), i. e.:

$$\Delta E_F = \frac{1}{4\pi^3} \operatorname{Im} \int \mathrm{d}^2\mathbf{k}_\parallel \int_{-\infty}^{+\infty} f(\varepsilon) \times \left[\ln\left(1 - r_\mathrm{A}^\uparrow r_\mathrm{B}^\uparrow \mathrm{e}^{\mathrm{i}q_\perp D}\right) + \ln\left(1 - r_\mathrm{A}^\downarrow r_\mathrm{B}^\downarrow \mathrm{e}^{\mathrm{i}q_\perp D}\right) \right] \mathrm{d}\varepsilon \tag{20}$$

In this equation the first and the second terms correspond, respectively, to majority- and minority-spin electrons. The antiferromagnetic conguration is obtained by reversing the magnetization of B, i. e. by interchanging $r_\mathrm{B}^\uparrow$ and $r_\mathrm{B}^\downarrow$; thus the corresponding energy per unit area is:

$$\Delta E_{AF} = \frac{1}{4\pi^3} \operatorname{Im} \int \mathrm{d}^2\mathbf{k}_\parallel \int_{-\infty}^{+\infty} f(\varepsilon) \times \left[\ln\left(1 - r_\mathrm{A}^\uparrow r_\mathrm{B}^\downarrow \mathrm{e}^{\mathrm{i}q_\perp D}\right) + \ln\left(1 - r_\mathrm{A}^\downarrow r_\mathrm{B}^\uparrow \mathrm{e}^{\mathrm{i}q_\perp D}\right) \right] \mathrm{d}\varepsilon \tag{21}$$

Thus, the interlayer exchange coupling energy is

$$E_F - E_{AF} = \frac{1}{4\pi^3} \operatorname{Im} \int \mathrm{d}^2\mathbf{k}_\parallel \int_{-\infty}^{+\infty} f(\varepsilon) \times \ln\left[\frac{\left(1 - r_\mathrm{A}^\uparrow r_\mathrm{B}^\uparrow \mathrm{e}^{\mathrm{i}q_\perp D}\right)\left(1 - r_\mathrm{A}^\downarrow r_\mathrm{B}^\downarrow \mathrm{e}^{\mathrm{i}q_\perp D}\right)}{\left(1 - r_\mathrm{A}^\uparrow r_\mathrm{B}^\downarrow \mathrm{e}^{\mathrm{i}q_\perp D}\right)\left(1 - r_\mathrm{A}^\downarrow r_\mathrm{B}^\uparrow \mathrm{e}^{\mathrm{i}q_\perp D}\right)} \right] \mathrm{d}\varepsilon \tag{22}$$

which can be simplified to:

$$E_F - E_{AF} \approx -\frac{1}{\pi^3} \operatorname{Im} \int \mathrm{d}^2\mathbf{k}_\parallel \int_{-\infty}^{\infty} f(\varepsilon)\, \Delta r_\mathrm{A} \Delta r_\mathrm{B}\, \mathrm{e}^{\mathrm{i}q_\perp D}\, \mathrm{d}\varepsilon \tag{23}$$

in the limit of weak confinement. The above expression for the IEC has a rather transparent physical interpretation. First, as the integrations on $\mathbf{k}_\parallel$ over the first two-dimensional Brillouin zone and on the energy up to the Fermi level show, the IEC is a sum of contributions from all occupied electronic states. The contribution of a given electronic state, of energy ε and in-plane wavevector $\mathbf{k}_\parallel$, consists of the product of three factors – the two factors Δr_A and Δr_B express the spin-asymmetry of the confinement, because of the magnetic layers A and B, respectively, whereas the exponential factor $\mathrm{e}^{\mathrm{i}q_\perp D}$ describes the propagation through the spacer and is responsible for the interference (or quantum-size) effect. Thus, this approach establishes

an explicit and direct link between oscillatory IEC and quantum size effects such as are observed in photoemission.

9.5 Asymptotic Behavior for Large Spacer Thicknesses

In the limit of large spacer thickness, D, the exponential factor oscillates rapidly with ε and $\mathbf{k}_\parallel$, which leads to substantial cancellation of the contributions to the IEC because of the different electronic states. Because the integration over energy is abruptly stopped at ε_F, however, states located at the Fermi level give predominant contributions. Thus the integral on ε can be calculated by fixing all other factors to their value at ε_F, and by expanding $q_\perp \equiv k_\perp^+ - k_\perp^-$ around ε_F, i. e.:

$$q_\perp \approx q_{\perp F} + 2\frac{\varepsilon - \varepsilon_F}{\hbar v_{\perp F}^{+-}}, \tag{24}$$

with:

$$\frac{2}{v_{\perp F}^{+-}} \equiv \frac{1}{v_{\perp F}^{+}} - \frac{1}{v_{\perp F}^{-}}. \tag{25}$$

The integration (see Ref. [74] for details) yields:

$$E_F - E_{AF} = \frac{1}{2\pi^3}\,\mathrm{Im}\int \mathrm{d}^2\mathbf{k}_\parallel \frac{i\hbar v_{\perp F}^{+-}}{D}\,\Delta r_A \Delta r_B e^{iq_{\perp F}D} \times F(2\pi\, k_B T\, D/\hbar v_{\perp F}^{+-}), \tag{26}$$

where:

$$F(x) \equiv \frac{x}{\sinh x}. \tag{27}$$

In the above equations, $q_{\perp F}$ is a vector spanning the *complex Fermi surface*; the velocity $v_{\perp F}^{+-}$ is a combination of the group velocities at the points $(\mathbf{k}_\parallel, k_{\perp F}^{+})$ and $(\mathbf{k}_\parallel, k_{\perp F}^{-})$ of the Fermi surface.

Next, the integration on $\mathbf{k}_\parallel$ is performed by noting that for large spacer thickness D the only significant contributions arise from the neighboring critical vectors $\mathbf{k}_\parallel^\alpha$ for which $q_{\perp F}$ is stationary. Around such vectors, $q_{\perp F}$ may be expanded as

$$q_{\perp F} = q_{\perp F}^\alpha - \frac{(k_x - k_x^\alpha)^2}{\kappa_x^\alpha} - \frac{\left(k_y - k_y^\alpha\right)^2}{\kappa_y^\alpha} \tag{28}$$

where the crossed terms have been canceled by proper choice of the x and y axes; κ_x^α and κ_y^α are combinations of the curvature radii of the Fermi surface at $(\mathbf{k}_\parallel^\alpha, k_\perp^{+\alpha})$ and $(\mathbf{k}_\parallel^\alpha, k_\perp^{-\alpha})$.

The integral is calculated by using the stationary phase approximation [74], and one obtains:

$$E_F - E_{AF} = \mathrm{Im} \sum_\alpha \frac{\hbar v_\perp^\alpha \kappa_\alpha}{2\pi^2 D^2} \Delta r_A^\alpha \Delta r_B^\alpha e^{iq_\perp^\alpha D} \times F(2\pi k_B T D/\hbar v_\perp^\alpha) \tag{29}$$

where $q_\perp^\alpha$, $v_\perp^\alpha$, Δr_A^α, Δr_B^α correspond to the critical vector $\mathbf{k}_\parallel^\alpha$, and:

$$\kappa_\alpha \equiv \left(\kappa_x^\alpha\right)^{1/2} \left(\kappa_y^\alpha\right)^{1/2} \tag{30}$$

in Eq. (30), one takes the square root with an argument between 0 and π.

This analysis shows that *in fine*, the only remaining contributions in the limit of large spacer thickness D arise from the neighborhood of states having in-plane wavevectors $\mathbf{k}_\parallel^\alpha$ such that the spanning vector of the Fermi surface $q_{\perp F} = k_{\perp F}^+ - k_{\perp F}^-$ is stationary with respect to $\mathbf{k}_\parallel$ for $\mathbf{k}_\parallel = \mathbf{k}_\parallel^\alpha$, and the corresponding contribution oscillates with a wavevector equal to $q_{\perp F}^\alpha$. This selection rule was first derived in the context of the RKKY model [117]; it is illustrated in Fig. 3. There may be several such stationary spanning vectors and, hence, several oscillatory components; they are labelled by the index α.

The above selection rule enables prediction of the dependence of the oscillation period(s) of the interlayer exchange coupling on spacer thickness, merely by inspecting the bulk Fermi surface of the spacer material. In view of an experimental test of these predictions, noble metal spacer layers seem to be the best suited candidates; there are several reasons for this choice:

- Fermi surfaces of noble metals are known very accurately from de Haas-van Alphen and cyclotron resonance experiments [116];
- because only the *sp* band intersects the Fermi level, the Fermi surface is rather simple, and does not depart very much from a free-electron Fermi sphere; and
- samples of very good quality with noble metals as a spacer layer could be prepared.

Fig. 4 shows a cross-section of the Fermi surface of Cu, indicating the stationary spanning vectors for the (001), (111), and (110) crystalline orientations [117]; the Fermi surfaces of Ag and Au are qualitatively similar. For the (111) orientation, a single (long) period is predicted; for the (001) orientation, both a long period and a

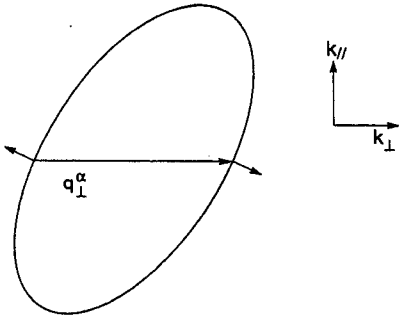

Fig. 3. Sketch showing the wavevector $q_\perp^\alpha$ giving the oscillation period of the oscillatory interlayer exchange coupling for a non-spherical Fermi surface.

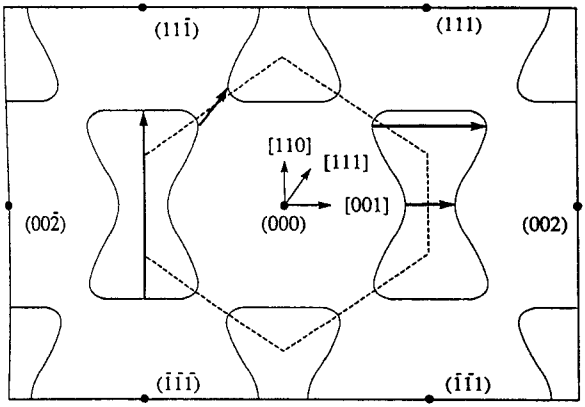

Fig. 4. Cross-section of the Fermi surface of Cu along the (1$\bar{1}$0) plane passing through the origin. The solid dots indicate the reciprocal lattice vectors. The dashed lines indicate the boundary of the first Brillouin zone. The horizontal, oblique, and vertical, solid arrows indicate the vectors $q_{\perp}^{\alpha}$ giving the oscillation period(s) for the (001), (111), and (110) orientations, respectively.

short period are predicted; for the (110) orientation, four different periods are predicted (only one stationary spanning vector is seen in Fig. 4, the three others being located in other cross-sections of the Fermi surface). These theoretical predictions have been confirmed successfully by numerous experimental observations. In particular, the coexistence of a long and a short period for the (001) orientation has been confirmed for Cu [20–22, 98, 122], Ag [23], and Au [17–19]; and the experimental periods have been found to be in excellent agreement with the theoretical predictions. Theoretically predicted and experimentally observed oscillation periods in Table 1.

Table 1. Comparison of the theoretical predictions of Ref. [117] with experimental observations of the dependence of oscillation periods of interlayer exchange coupling on spacer thickness.

Spacer	Theoretical periods	System	Experimental periods	Ref.
Cu(111)	$\Lambda = 4.5$ AL	Co/Cu/Co(111)	$\Lambda \approx 5.$ AL	[118]
		Co/Cu/Co(111)	$\Lambda \approx 6.$ AL	[119]
		Fe/Cu/Fe(111)	$\Lambda \approx 6.$ AL	[120]
Cu(001)	$\Lambda_1 = 2.6$ AL	Co/Cu/Co(001)	$\Lambda \approx 6.$ AL	[121]
	$\Lambda_2 = 5.9$ AL	Co/Cu/Co(001)	$\Lambda_1 \approx 2.6$ AL	[20]
			$\Lambda_2 \approx 8.$ AL	
		Co/Cu/Co(001)	$\Lambda_1 \approx 2.7$ AL	[22]
			$\Lambda_2 \approx 6.1$ AL	
		Fe/Cu/Fe(001)	$\Lambda \approx 7.5$ AL	[106]
Ag(001)	$\Lambda_1 = 2.4$ AL	Fe/Ag/Fe(001)	$\Lambda_1 \approx 2.4$ AL	[23]
	$\Lambda_2 = 5.6$ AL		$\Lambda_2 \approx 5.6$ AL	
Au(001)	$\Lambda_1 = 2.5$ AL	Fe/Au/Fe(001)	$\Lambda_1 \approx 2.$ AL	[17]
	$\Lambda_2 = 8.6$ AL		$\Lambda_2 \approx 7$–8 AL	
		Fe/Au/Fe(001)	$\Lambda_1 \approx 2.5$ AL	[18, 19]
			$\Lambda_2 \approx 8.6$ AL	
Au(111)	$\Lambda = 4.8$ AL	Co/Au/Co(111)	$\Lambda \approx 4.5$ AL	[14]

In a further attempt to test theoretical predictions of the periods of oscillatory coupling, several groups [123–125] have undertaken to modify, in a controlled manner, the size of the Fermi surface (and hence, the period of the coupling) by alloying the spacer noble metal (Cu) with a metal of lower valence (Ni); in both experiments, the change in oscillation period as a result of alloying has been found to be in good agreement with the expected change in the Fermi surface.

9.6 Effect of Magnetic Layer Thickness

As already mentioned, the influence of the IEC on the ferromagnetic layer thickness is contained in the reflection coefficients Δr_A and Δr_B. If the ferromagnetic layers are of finite thickness, reflections usually occur at the two interfaces bounding the ferromagnetic layers, giving rise to interferences [61] and, hence, to oscillations of the IEC which depend on ferromagnetic layer-thickness. A more detailed discussion of this effect is given in Refs. [74, 61]. This behavior was first predicted from calculations based on a free-electron model [126]. The dependence of the amplitude of the oscillations of the IEC on ferromagnetic layer-thickness is generally much smaller than the dependence on spacer thickness, and does not give rise to changes of the sign of the IEC. Experimentally this effect was confirmed by Bloemen et al. [24] for Co/Cu/Co(001) and by Back et al. [25] for Fe/Cu/Co(001). It has also been confirmed theoretically by Nordström et al. [127], Lang et al. [128], Drchal et al. [129], and Lee and Chang [59].

9.7 Effect of Overlayer Thickness

More surprising behavior (at first sight) is the dependence of the IEC on the thickness of an external overlayer. One might naïely believe that layers external to the basic ferromagnet/spacer/ferromagnet sandwich should not influence the interaction between the two ferromagnetic layers. This view is incorrect, in particular when the system is covered by an ultrathin protective overlayer. In these circumstances, the electrons can to reach the vacuum barrier, which is perfectly reflecting, so that strong confinement and interference effects occur in the overlayer; this leads to weak but significant oscillatory variation of the IEC as a function of the overlayer thickness [62].

This effect, which follows directly from the quantum interference (or quantum size-effect) mechanism, has been proposed and experimentally confirmed independently by de Vries et al. [26] for the Co/Cu/Co(001) system with a Cu(001) overlayer, by Okuno and Inomata [27] for the Fe/Au/Fe(001) system with an Au(001) overlayer, and by Bounouh et al. [28] for Co/Au/Co(0001) with an Au(111) overlayer. In all this work, the dependence of the observed period(s) of the oscillations on overlayer

Table 2. Comparison of theoretical predictions of Ref. [62] and experimental observations of the dependence of the oscillation periods of interlayer exchange coupling overlayer thickness.

Overlayer	Theoretical periods	System	Experimental periods	Ref.
Cu(001)	$\Lambda_1 = 2.6$ AL $\Lambda_2 = 5.9$ AL	Cu/Co/Cu/Co/Cu(001)	$\Lambda \approx 5.$ AL	[26]
Au(001)	$\Lambda_1 = 2.5$ AL $\Lambda_2 = 8.6$ AL	Au/Fe/Au/Fe/Au(001)	$\Lambda_1 \approx 2.6$ AL $\Lambda_2 \approx 8.0$ AL	[27]
Au(111)	$\Lambda = 4.8$ AL	Au/Co/Au/Co/Au(111)	$\Lambda \approx 5.$ AL	[28]

thickness were found to be in good agreement with theoretically predicted values. This effect has also been confirmed by means of first-principles calculations for the Co/Cu/Co(001) system with different types of overlayer [130–132]. The dependence of the oscillation periods on overlayer thickness predicted theoretically are compared with those observed experimentally in Table 2. A more detailed discussion of this effect can be found in Refs. [62, 130, 132].

9.8 Strength and Phase of Interlayer Exchange Coupling

In contrast with the excellent agreement between theory and experiment obtained for oscillation periods, the situation for the amplitude and phase of oscillations is less satisfactory. According to the theory expounded above, the coupling takes the following form in the limit of large spacer thickness (asymptotic limit):

$$J = \sum_{\alpha} \frac{A_\alpha}{D^2} \sin(q_\alpha D + \phi_\alpha) . \tag{31}$$

Because the coupling constant J has the dimension of energy per unit area, the parameters A_α characterizing the coupling strength of the different components of the oscillation have the dimensions of energy. By taking typical values of the Fermi wavevector and velocity, it is easy to see from Eq. (29) that they are typically of the order of 1 to 10 meV.

Theoretical and experimental values of the oscillation amplitude strengths, A_α, for different systems are compared in Table 3. (Note that different theoretical results with each other we include in this discussion only calculations pertaining to semi-infinite magnetic layers.) We observe a variety of rather strong discrepancy between theory and experiment, and also among various theoretical studies. Although the agreement seems to be rather good for the Co/Cu(111)/Co system, more experimental and theoretical data are required to disclose whether the apparent agreement is conclusive or accidental.

Table 3. Comparison of theoretical predictions and experimental observations for the dependence of oscillation amplitudes, A_α, of interlayer exchange coupling on spacer thickness. For Cu(001) and Au(001) spacers A_1 and A_2 correspond, respectively, to the short-period and long-period oscillations.

System	Theory	Ref.	Experiment	Ref.
Co/Cu(111)/Co	$A \approx 3.7$ meV	[133]	$A \approx 7.6$ meV	[20]
	$A \approx 4.2$ meV	[60]	$A \approx 3.4$ meV	[137]
			$A \approx 2.5$ meV	[138]
Co/Cu(001)/Co	$A_1 \approx 42.$ meV	[133]	$A_1 \approx 1.6$ meV	[20, 21, 122]
	$A_2 \approx 0.13$ meV		$A_2 \approx 1.4$ meV	
	$A_1 \approx 72.$ meV	[60]		
	$A_2 \approx 0.75$ meV			
	$A_1 \approx 35.$ meV	[129]		
	$A_2 \approx 3.5$ meV			
	$A_1 \approx 35.$ meV	[47]		
	$A_2 \approx 0.035$ meV			
Fe/Au(001)/Fe	$A_1 \approx 12.5$ meV	[60]	$A_1 \approx 8.1$ meV	[19]
	$A_2 \approx 6.9$ meV		$A_2 \approx 1.1$ meV	

9.8.1 Co/Cu(001)/Co

The Co/Cu(001)/Co system has been most investigated theoretically and is considered to be a model system to test the predictions of theory. The theoretical results reported in Table 3 correspond to semi-infinite magnetic layers, whereas the experimental data have been obtained for magnetic layers of finite thickness. As discussed in Section 6 the strength of the coupling varies with magnetic layer thickness, which can be a source of discrepancy between theoretical and experimental results. Another possible source of discrepancy arises from unavoidable imperfections (roughness, intermixing) of the experimental samples.

Let us first address the short-period oscillatory component (labeled with the subscript 1). As discussed in Section 5 above, this component arises from four equivalent in-plane wavevectors $\mathbf{k}_{\parallel 1}$ located on the $\overline{\Gamma} - \overline{X}$ high-symmetry line of the two-dimensional Brillouin zone [74]. Because the majority-spin band structure of fcc Co well matches that of Cu, $|r_1^{\uparrow}| \approx 0$. For minority-spin fcc Co, on the other hand, there is a local gap in the band structure of symmetry compatible with the Cu states, which leads to total reflection, i. e., $|r_1^{\downarrow}| = 1$. Thus, $|\Delta r_1| \approx 0.5$ [133, 134] and $|\Delta r_1|$ is (almost) independent of Co thickness [129]. The various theoretical values for the amplitude A_1 listed in Table 3 agree rather well with each other, except for that from Ref. [60] which is almost a factor of 2 larger than the values obtained by other authors [129, 133, 47]. This discrepancy might be because of an error in the estimation of the radius of curvature κ_1, of the Fermi surface, and of the Fermi velocity, $v_{\perp 1}$, which are quite tricky to obtain accurately for $\mathbf{k}_{\parallel 1}$.

Turning now to the comparison between theory and experiment, we notice that the calculated values of A_1 are considerably larger than those measured. There might be

at least two reasons for this discrepancy. The first is the effect of interface roughness, which generally tends to reduce the amplitude of the coupling oscillations [117]; this effect is particularly pronounced for short-period oscillatory components, as is indeed confirmed experimentally [22]. The second reason is of intrinsic character – the theoretical values of A_1 given in Table 3 correspond to the asymptotic limit, whereas the experimental data have been obtained for spacer thicknesses below 15 AL. As is clearly apparent from Fig. 6a of Ref. [129] and from Fig. 13 (bottom) of Ref. [47], the asymptotic regime is attained only for thicknesses above 20 to 40 AL; below this value the envelope of the oscillations deviates significantly from D^{-2} behavior, and the apparent amplitude in the range relevant to experiments is typically a factor of 2 smaller than the asymptotic amplitude. This pre-asymptotic correction is attributed to the strong energy-dependence of $r_1^{\downarrow}$ [47].

Let us now discuss the long-period oscillatory component. As appears from Table 3, the situation is quite confusing – not only do the various theoretical results disagree with each other, but some [133, 60, 47] *underestimate* the coupling strength compared with the experimental result [20, 21, 122], a difference which cannot be explained by the effect of roughness or interdiffusion.

The long-period oscillatory component arises from the center $\overline{\Gamma}$ of the two-dimensional Brillouin zone. Here again, for the same reason as above, $|r_2^{\uparrow}| \approx 0$. The minority-spin reflection coefficient, is on the other hand, considerably smaller than for the short-period oscillation, and $|r_2^{\downarrow}| \approx 0.15$ [74], so that $|\Delta r_2| \approx 0.05$ [74, 133]. This very small spin-dependent confinement explains the very small values of A_2 obtained by authors who rely on the asymptotic expression, Eq. (29), obtained from the stationary phase approximation [133, 60, 47]. As seen from Fig. 2 of Ref. [135] and from Fig. 2 of Ref. [60], however, $r_2^{\downarrow}$ increases very strongly with $\mathbf{k}_{\parallel}$ and full reflection is reached at a distance $0.1 \times \pi/a$ from $\overline{\Gamma}$; indeed, the low reflectivity arises only in a narrow window around $\overline{\Gamma}$. As discussed in Ref. [136], this gives rise to a strong preasymptotic correction, and explains why the stationary-phase approximation yields an *underestimated* value of A_2. If, on the other hand, the $\mathbf{k}_{\parallel}$ integration is performed without using the stationary-phase approximation, as in Ref. [129], a much higher value of A_2 is obtained; the latter is larger than the experimental value [20, 21, 122] by a factor of 2.5, which seems plausible in view of the effect of roughness and interdiffusion.

Our knowledge of the phase of the oscillations is much more restricted as this aspect of the problem has so far attracted little attention, with the notable exception of the work of Weber et al. [22]. On general grounds, for total reflection (as for $r_{1\downarrow}$), one expects the phase to vary with magnetic layer thickness and/or with the chemical nature of the magnetic layer; conversely, for weak confinement (as for $r_2^{\downarrow}$), one expects the phase to be almost invariant [74]. These general trends were, indeed, confirmed experimentally by Weber et al. [22].

9.8.2 Fe/Au(001/Fe

Because of the excellent lattice matching between Au and bcc Fe (with rotation of the cubic axes of the latter by 45°), and the availability of extremely smooth Fe substrates (whiskers) [18, 19], Fe/Au(001)/Fe is an excellent system for a quantitative testing of theory.

In contrast with Co/Cu(001) discussed above, for Fe/Au(001) one has total reflection of minority-spin electrons both at $\mathbf{k}_{\parallel 1}$ (short-period oscillation) and $\mathbf{k}_{\parallel 2}$ (long-period oscillation), and $|r^{\downarrow}|$ is almost independent of $\mathbf{k}_{\parallel}$ around these points, as is clearly apparent from Fig. 1 of Ref. [134]. The associated preasymptotic correction should, therefore, not be very strong.

Indeed, as is apparent from Table 3, the predicted amplitudes are quite large, both for the short-period and long-period oscillatory components [60]. These predictions are fairly well confirmed by state-of-the-art experimental studies [19], although the predicted amplitude of the long-period component is too large by a factor of 6.

Clearly, even for this almost ideal system, further work is required to achieve satisfactory quantitative agreement between theory and experiment.

9.9 Concluding Remarks

As has been discussed in detail in this review, there is much experimental evidence that the mechanism of quantum confinement presented above is actually appropriate for explaining the phenomenon of oscillatory interlayer exchange coupling. This mechanism is entirely based upon a picture of independent electrons. This might seem paradoxical at first sight, because exchange interactions are ultimately a result of Coulomb interaction between electrons. This independent-electron picture can in fact be, justified theoretically and is based upon the "magnetic force theorem." A thorough discussion of this fundamental (but somewhat technical) aspect of the problem is given elsewhere [139, 140].

Despite the successes of the quantum confinement mechanism, several questions remain to be clarified for full understanding of the phenomenon. In particular, the validity of the asymptotic expression (29) must be assessed more quantitatively than has been achieved so far; a first attempt at addressing this issue is given in Ref. [136].

Acknowledgements

I am grateful to Claude Chappert, Josef Kudrnovský, Vaclav Drchal, and Ilja Turek for their collaboration in the work presented in this chapter.

References

[1] L. Néel, *C. R. Acad. Sci. (Paris)* **255**, 1545 (1962); *C. R. Acad. Sci. (Paris)* **255**, 1676 (1962).
[2] M.A. Ruderman and C. Kittel, *Phys. Rev.* **96**, 99 (1954).
[3] T. Kasuya, *Prog. Theor. Phys.* **16**, 45 (1956).
[4] K. Yosida, Phys. Rev. **106**, 893 (1957).
[5] C.F. Majkrzak, C.W. Cable, J. Kwo, M. Hong, B.D. McWhan, Y. Yafet, J.V. Waszak, and C. Vettier, *Phys. Rev. Lett.* **56**, 2700 (1986).
[6] M.B. Salamon, S. Sinha, J.J. Rhyne, J.E. Cunningham, R.W. Erwin, J. Borchers, and C.P. Flynn, *Phys. Rev. Lett.* **56**, 259 (1986).
[7] C.F. Majkrzak, J. Kwo, M. Hong, Y. Yafet, D. Gibbs, C.L. Chein, and J. Bohr, *Adv. Phys.* **40**, 99 (1991).
[8] J.J. Rhyne and R.W. Erwin, in *Magnetic Materials*, Vol. 8, Ed. K.H.J. Buschow, North Holland, Amsterdam, 1995, p. 1.
[9] P. Grünberg, R. Schreiber, Y. Pang, M.B. Brodsky, and H. Sower, *Phys. Rev. Lett.* **57**, 2442 (1986).
[10] B. Dieny, J.-P. Gavigan, and J.-P. Rebouillat, *J. Phys.: Condens. Matter* **2**, 159 (1990); B. Dieny and J.-P. Gavigan, *J. Phys.: Condens. Matter* **2**, 178 (1990).
[11] W. Folkerts, *J. Magn. Magn. Mater.* **94**, 302 (1990).
[12] B. Dieny, V.S. Speriosu, S.S.P. Parkin, and B.A. Gurney, *Phys. Rev. B* **43**, 1297 (1991).
[13] S.S.P. Parkin and D. Mauri, *Phys. Rev. B* **44**, 7131 (1991).
[14] V. Grolier, D. Renard, B. Bartenlian, P. Beauvillain, C. Chappert, C. Dupas, J. Ferré, M. Galtier, E. Kolb, M. Mulloy, J.P. Renard, and P. Veillet, *Phys. Rev. Lett.* **71**, 3023 (1993).
[15] S.S.P. Parkin, N. More, and K.P. Roche, *Phys. Rev. Lett.* **64**, 2304 (1990).
[16] S.S.P. Parkin, *Phys. Rev. Lett.* **67**, 3598 (1991).
[17] A. Fuss, S. Demokritov, P. Grünberg, and W. Zinn, *J. Magn. Magn. Mater.* **103**, L221 (1992).
[18] J. Unguris, R.J. Celotta, and D.T. Pierce, *J. Appl. Phys.* **75**, 6437 (1994).
[19] J. Unguris, R.J. Celotta, and D.T. Pierce, *Phys. Rev. Lett.* **79**, 2734 (1997)
[20] M.T. Johnson, S.T. Purcell, N.W.E. McGee, R. Coehoorn, J. aan de Stegge, and W. Hoving, *Phys. Rev. Lett.* **68**, 2688 (1992).
[21] M.T. Johnson, P.J.H. Bloemen, R. Coehoorn, J.J. de Vries, N.W.E. McGee, R. Jungblut, A. Reinders, and J. aan de Stegge, *Mat. Res. Soc. Proc.*, Vol. 313, Materials Research Society, San Francisco, 1993, p. 93.
[22] W. Weber, R. Allenspach, and A. Bischof, *Europhys. Lett.* **31**, 491 (1995).
[23] J. Unguris, R.J. Celotta, and D.T. Pierce, *J. Magn. Magn. Mater.* **127**, 205 (1993).
[24] P.J.H. Bloemen, M.T. Johnson, M.T.H. van de Vorst, R. Coehoorn, J.J. de Vries, R. Jungblut, J. aan de Stegge, A. Reinders, and W.J.M. de Jonge, *Phys. Rev. Lett.* **72**, 764 (1994).
[25] C.H. Back, W. Weber, A. Bischof, D. Pescia, and R. Allenspach, *Phys. Rev. B* **52** R13114 (1995).
[26] J.J. de Vries, A.A.P. Schudelaro, R. Jungblut, P.J.H. Bloemen, A. Reinders, J. Kohlhepp, R. Coehoorn, and de W.J.M. Jonge, *Phys. Rev. Lett.* **75**, 1306 (1995).
[27] S.N. Okuno and K. Inomata, *J. Phys. Soc. Japan* **64**, 3631 (1995).
[28] A. Bounouh, P. Beauvillain, P. Bruno, C. Chappert, R. Mégy, and P. Veillet, *Europhys. Lett.* **33**, 315 (1996).
[29] M. Rührig, R. Schäfer, A. Hubert, R. Mosler, J.A. Wolf, S. Demokritov, and P. Grünberg, *Phys. Status Solidi A* **125**, 635 (1991).

[30] J.C. Slonczewski, *J. Magn. Magn. Mater.* **150**, 13 (1995).
[31] S.O. Demokritov, *J. Phys. D: Appl. Phys.* **31**, 925 (1998).
[32] S. Toscano, B. Briner, H. Hopster, and M. Landolt, *J. Magn. Magn. Matter.* **114**, L6 (1992).
[33] S. Toscano, B. Briner, and M. Landolt, in *Magnetism and Structure in Systems of Reduced Dimensions*, Ed. R.F.C. Farrow, B. Dieny, M. Donath, A. Fert, and B.D. Hermsmeier, Vol. 309 of *NATO Advanced Study Institute, Series B: Physics*, Plenum Press, New York, 1993, p. 257.
[34] J.E. Mattson, S. Kumar, E.E. Fullerton, S.R. Lee, C.H. Sowers, M. Grimditch, S.D. Bader, and F.T. Parker, *Phys. Rev. Lett.* **71**, 185 (1993).
[35] B. Briner and M. Landolt, *Phys. Rev. Lett.* **73**, 340 (1994).
[36] Y. Yafet, *Phys. Rev. B* **36**, 3948 (1987).
[37] C. Chappert and J.P. Renard, *Europhys. Lett.* **15**, 553 (1991).
[38] P. Bruno and C. Chappert, *Phys. Rev. Lett.* **67**, 1602 (1991); **67**, 2592(E) (1991).
[39] P. Bruno and C. Chappert, *Phys. Rev. B* **46**, 261 (1992).
[40] R. Coehoorn, *Phys. Rev. B* **44**, 9331 (1991).
[41] D.M. Edwards, J. Mathon, R.B. Muniz, and M.S. Phan, *Phys. Rev. Lett.* **67**, 493 (1991).
[42] J. Mathon, M. Villeret, and D.M. Edwards, *J. Phys.: Condens. Mat.* **4**, 9873 (1992).
[43] J. Barnaś, *J. Magn. Magn. Mater.* **111**, L215 (1992).
[44] R.P. Erickson, K.B. Hathaway, and J.R. Cullen, *Phys. Rev. B* **47**, 2626 (1993).
[45] J.C. Slonczewski, *J. Magn. Magn. Mater.* **126**, 374 (1993).
[46] J. d'Albuquerque e Castro, J. Mathon, M. Villeret, and A. Umerski, *Phys. Rev. B* **53**, R13306 (1996).
[47] J. Mathon, M. Villeret, A. Umerski, R.B. Muniz, J. d'Albuquerque e Castro, and D.M. Edwards, *Phys. Rev. B* **56**, 11797 (1997).
[48] A.T. Costa, Jr., J. d'Albuquerque e Castro, and R.B. Muniz, *Phys. Rev. B* **56**, 13697 (1997).
[49] Y. Wang, P.M. Levy, and J.L. Fry, *Phys. Rev. Lett.* **65**, 2732 (1990).
[50] Z.P. Shi, P.M. Levy, and J.L. Fry, *Phys. Rev. Lett.* **69**, 3678 (1992).
[51] P. Bruno, *J. Magn. Magn. Mater.* **116**, L13 (1992).
[52] P.W. Anderson, *Phys. Rev.* **124**, 41 (1961).
[53] B. Caroli, *J. Phys. Chem. Solids* **28**, 1427 (1967).
[54] J. Friedel, *Nuovo Cimento Suppl.* **7**, 287 (1958).
[55] P. Bruno, *J. Magn. Magn. Mater.* **121**, 248 (1993).
[56] P. Bruno, *Phys. Rev. B* **52**, 411 (1995).
[57] M.D. Stiles, *Phys. Rev. B* **48** 7238 (1193).
[58] B. Lee and Y.-C. Chang, *Phys. Rev. B* **52**, 3499 (1995).
[59] B. Lee and Y.C. Chang, *Phys. Rev. B* **54**, 13034 (1996).
[60] M.D. Stiles, *J. Appl. Phys.* **79**, 5805 (1996).
[61] P. Bruno, *Europhys. Lett.* **23**, 615 (1993).
[62] P. Bruno, *J. Magn. Magn. Mater.* **164**, 27 (1996).
[63] F. Herman, J. Sticht, and M. van Schilfgaarde, *J. Appl. Phys.* **69**, 4783 (1991); in *Magnetic Thin Films, Multilayers and Surfaces*, Ed. S.S.P. Parkin, H. Hopster, J.P. Renard, T. Shinjo, and W. Zinn, Symposia Proceedings No. 231, Materials Research Society, Pittsburg, 1992.
[64] S. Krompiewski, U. Krey, and J. Pirnay, *J. Magn. Magn. Mater.* **121**, 238 (1993).
[65] S. Krompiewski, F. Süss, and U. Krey, *Europhys. Lett.* **26**, 303 (1994).
[66] M. van Schilfgaarde and F. Herman, *Phys. Rev. Lett.* **71**, 1923 (1993).
[67] P. Lang, L. Nordström, R. Zeller, and P.H. Dederichs, *Phys. Rev. Lett.* **71**, 1927 (1993).
[68] L. Norström, P. Lang, R. Zeller, and P.H. Dederichs, *Phys. Rev. B* **50**, 13058 (1994).
[69] J. Kudrnovský, V. Drchal, I. Turek, and P. Weinberger, *Phys. Rev. B* **50**, 16105 (1994).
[70] J. Kudrnovský, V. Drchal, I. Turek, M. Šob, and P. Weinberger, *Phys. Rev. B* **53**, 5125 (1996).

[71] P. Lang, L. Nordström, K. Wildberger, R. Zeller, P.H. Dederichs, and T. Hoshino, *Phys. Rev. B* **53**, 9092 (1996).
[72] V. Drchal, J. Kudrnovský, I. Turek, and P. Weinberger, *Phys. Rev. B* **53**, 15036 (1996).
[73] P. Bruno, *Phys. Rev. B* **49**, 13231 (1994).
[74] P. Bruno, *Phys. Rev. B* **52**, 411 (1995).
[75] P.D. Loly and J.B. Pendry, *J. Phys. C: Solid State Phys.* **16**, 423 (1983).
[76] A.L. Wachs, A.P. Shapiro, T.C. Hsieh, and T.-C. Chiang, *Phys. Rev. B* **33**, 1460 (1986).
[77] S.Å Lindgren and L. Walldén, *Phys. Rev. Lett.* **59**, 3003 (1987).
[78] S.Å Lindgren and L. Walldén, *Phys. Rev. Lett.* **61**, 2894 (1988).
[79] S.Å Lindgren and L. Walldén, *Phys. Rev. B* **38**, 3060 (1988).
[80] S.Å Lindgren and L. Walldén, *J. Phys.: Condens. Matter* **1**, 2151 (1989).
[81] T. Miller, A. Samsavar, G.E. Franklin, and T.-C. Chiang, *Phys. Rev. Lett.* **61**, 1404 (1988).
[82] M.A. Mueller, A. Samsavar, T. Miller, and T.-C. Chiang, *Phys. Rev. B* **40**, 5845 (1989).
[83] M.A. Mueller, T. Miller, and T.-C. Chiang, *Phys. Rev. B* **41**, 5214 (1990).
[84] M. Jalochowski, E. Bauer, H. Knoppe, and G. Lilienkamp, *Phys. Rev. B* **45**, 13607 (1992).
[85] N.B. Brookes, Y. Chang, and P.D. Johnson, *Phys. Rev. Lett.* **67**, 354 (1991).
[86] J.E. Ortega and F.J. Himpsel, *Phys. Rev. Lett.* **69**, 844 (1992).
[87] J.E. Ortega, F.J. Himpsel, G.J. Mankey, and R.F. Willis, *Phys. Rev. B* **47**, 1540 (1993).
[88] J.E. Ortega, F.J. Himpsel, G.J. Mankey, and R.F. Willis, *J. Appl. Phys.* **73**, 5771 (1993).
[89] K. Garrison, Y. Chang, and P.D. Johnson, *Phys. Rev. Lett.* **71**, 2801 (1993).
[90] C. Carbone, E. Vescovo, O. Rader, W. Gudat, and W. Eberhardt, *Phys. Rev. Lett.* **71**, 2805 (1993).
[91] N.V. Smith, N.B. Brookes, Y. Chang, and P.D. Johnson, *Phys. Rev. B* **49**, 332 (1994).
[92] P.D. Johnson, K. Garrison, Q. Dong, N.V. Smith, D. Li, J. Mattson, J. Pearson, and S.D. Bader, *Phys. Rev. B* **50**, 8954 (1994).
[93] F.J. Himpsel and O. Rader, *Appl. Phys. Lett.* **67**, 1151 (1995).
[94] S. Crampin, S. De Rossi, and F. Ciccaci, *Phys. Rev. B* **53**, 13817 (1996).
[95] P. Segovia, E.G. Michel, and J.E. Ortega, *Phys. Rev. Lett.* **77**, 3455 (1996).
[96] R. Kläsge, D. Schmitz, C. Carbone, W. Eberhardt, P. Lang, R. Zeller, and P.H. Dederichs, *Phys. Rev. B* **57**, R696 (1998).
[97] R.K. Kawakami, E. Rotenberg, E.J. Escocia-Aparicio, H.J. Choi, T.R. Cummins, J.G. Tobin, N.V. Smith, Z.Q. and Qiu, *Phys. Rev. Lett.* **80**, 1754 (1998).
[98] R.K. Kawakami, E. Rotenberg, E.J. Escocia-Aparicio, H.J. Choi, J.H. Wolfe, N.V. Smith, and Z.Q. Qiu, *Phys. Rev. Lett.* **82**, 4098 (1999).
[99] F.J. Himpsel, *Phys. Rev. B* **44**, 5966 (1991).
[100] J.E. Ortega and F.J. Himpsel, *Phys. Rev. B* **47**, 16441 (1993).
[101] D. Li, J. Pearson, J.E. Mattson, S.D. Bader, and P.D. Johnson, *Phys. Rev. B* **51**, 7195 (1995).
[102] F.J. Himpsel, *J. Electr. Microsc. and Rel. Phenom.* **75**, 187 (1995).
[103] D. Li, J. Pearson, S.D. Bader, E. Vescovo, D.-J. Huang, P.D. Johnson, and B. Heinreich, *Phys. Rev. Lett.* **78**, 1154 (1997).
[104] K. Koike, T. Furukawa, G.P. Cameron, and Y. Murayama, *Phys. Rev. B* **50**, 4816 (1994).
[105] T. Furukawa and K. Koike, *Phys. Rev. B* **54**, 17896 (1996).
[106] W.R. Bennett, W. Schwarzacher, and W.F. Egelhoff, Jr., *Phys. Rev. Lett.* **65**, 3169 (1990).
[107] T. Katayama, Y. Suzuki, M. Hayashi, and A. Thiaville, *J. Magn. Magn. Mater.* **126**, 527 (1993).
[108] A. Carl and D. Weller, *Phys. Rev. Lett.* **74**, 190 (1995).
[109] R. Mégy, A. Bounouh, Y. Suzuki, P. Beauvillain, P. Bruno, C. Chappert, B. Lécuyer, and P. Veillet, *Phys. Rev. B* **51**, 5586 (1995).
[110] P. Bruno, Y. Suzuki and C. Chappert, *Phys. Rev. B* **53**, 9214 (1996).

[111] Y. Suzuki, T. Katayama, P. Bruno, S. Yuasa, and E. Tamura, *Phys. Rev. Lett.* **80**, 5200 (1998).
[112] T.A. Luce, W. Hübner, and K.H. Bennemann, *Phys. Rev. Lett.* **77**, 2810 (1996).
[113] A. Kirilyuk, Th. Rasing, R. Mégy, and P. Beauvillain, *Phys. Rev. Lett.* **77**, 4608 (1996).
[114] W. Weber, A. Bischof, R. Allenspach, C. Würsch, C.H. Back, and D. Pescia, *Phys. Rev. Lett.* **76**, 3424 (1996).
[115] C.H. Back, W. Weber, C. Würsch, A. Bischof, D. Pescia, and R. Allespach, *J. Appl. Phys.* **81**, 5054 (1997).
[116] M.R. Halse, *Philos. Trans. R. Soc. London A* **265**, 507 (1969).
[117] P. Bruno and C. Chappert, *Phys. Rev. Lett.* **67**, 1602 (1991); **67**, 2592(E) (1991).
[118] S.S.P. Parkin, R. Bhadra, and K.P. Roche, *Phys. Rev. Lett.* **66**, 2152 (1991).
[119] D.H. Mosca, F. Pétroff, A. Fert, P.A. Schroeder, W.P. Pratt, Jr., R. Laloee, and S. Lequien, *J. Magn. Magn. Mater.* **94**, L1 (1991).
[120] F. Pétroff, A. Barthéémy, D.H. Mosca, D.K. Lottis, A. Fert, P.A. Schroeder, W.P. Pratt, Jr., R. Laloee, and S. Lequien, *Phys. Rev. B* **44**, 5355 (1991).
[121] J.J. de Miguel, A. Cebollada, J.M. Gallego, R. Miranda, C.M. Schneider, P. Schuster, and J. Kirschner, *J. Magn. Magn. Mater.* **93**, 1 (1991).
[122] J.J. de Vries, PhD Thesis, Eindhoven University of Technology (1996).
[123] S.N. Okuno and K. Inomata, *Phys. Rev. Lett.* **70**, 1771 (1993).
[124] S.S.P. Parkin, C. Chappert, and F. Herman, *Europhys. Lett.* **24**, 71 (1993).
[125] J.-F. Bobo, L. Hennet, and M. Piécuch, *Europhys. Lett.* **24**, 139 (1993).
[126] J. Barnaś, *J. Magn. Magn. Mater.* **111**, L215 (1992).
[127] L. Norström, P. Lang, R. Zeller, and P.H. Dederichs, *Phys. Rev. B* **50**, 13058 (1994).
[128] P. Lang, L. Nordström, K. Wildberger, R. Zeller, P.H. Dederichs, and T. Hoshino, *Phys. Rev. B* **53**, 9092 (1996).
[129] V. Drchal, J. Kudrnovský, I. Turek, and P. Weinberger, *Phys. Rev. B* **53**, 15036 (1996).
[130] J. Kudrnovský, V. Drchal, P. Bruno, I. Turek, and P. Weinberger, *Phys. Rev. B.* **56**, 8919 (1997).
[131] J. Kudrnovský, V. Drchal, P. Bruno, R. Coehoorn, J.J. de Vries, and P. Weinberger, *Mater Res. Soc. Symp. Proc. Vol.* **475**, 575 (1997).
[132] J. Kudrnovský, V. Drchal, P. Bruno, I. Turek, and P. Weinberger, *Comp. Matter Sci.* **10** 188 (1998).
[133] B. Lee and Y.-C. Chang, *Phys. Rev. B* **52**, 3499 (1995).
[134] M.D. Stiles, *J. Magn. Magn. Mater.* **200**, 322 (1999).
[135] P. Bruno, *J. Magn. Magn. Mater.* **148**, 202 (1995).
[136] P. Bruno, *Eur. Phys. J. B* **11**, 83 (1999).
[137] A. Schreyer, K. Bröhl, J.F. Ankner, C.F. Majkrzak, T. Zeidler, P. Bödeker, N. Metoki, and H. Zabel, *Phys. Rev. B* **47**, 15334 (1993).
[138] A.J.R. Ives, R.J. Hicken, J.A.C. Bland, C. Daboo, M. Gester, and S.J. Gray, *J. Appl. Phys.* **75**, 6458 (1994).
[139] P. Bruno, in *Magnetische Schichtsysteme*, Ed. P.H. Dederichs and P. Gruenberg, Forschungszentrum Jülich, 1999, Chap. B8; cond-mat/9905022.
[140] P. Bruno, *Eur. Phys. J. B* **11**, 83 (1999).